



Injection moulding of micropillar arrays: a comparison of poly(methyl methacrylate) and cyclic olefin copolymer

Bin Guan¹ · Jing-Hong Pai² · Mark Cherrill² · Billy Michalatos² · Craig Priest^{1,2}

Received: 8 January 2022 / Accepted: 15 July 2022 / Published online: 3 August 2022
© The Author(s) 2022

Abstract

Injection moulding of micropillar arrays offers a fast and inexpensive method for manufacturing sensors, optics, lab-on-a-chip devices, and medical devices. Material choice is important for both the function of the device and manufacturing optimisation. Here, a comparative study of poly(methyl methacrylate) (PMMA) and cyclic olefin copolymer (COC) injection moulding of micropillar arrays is presented. These two polymers are chosen for their convenient physical, chemical, and optical properties, which are favoured for microfluidic devices. COC is shown to replicate the mould's nano/microstructures more precisely than PMMA. COC successfully forms a micropillar array (250 nm diameter; 496 nm high) and closely replicates surfaces with nano-scale roughness (30–120 nm). In the same moulds, PMMA forms lens arrays (not true pillars) and smoother surfaces due to the incomplete filling for all parameters studied. Thus, COC offers finer structural detail for devices that require micro and nano-structured features, and may be more suited to injection moulding microfluidic devices.

1 Introduction

Micropillar arrays as a value-adding component in microfluidic chips have enabled a wide range of advanced applications, including sensing (Chen et al. 2020), diagnosis (Li et al. 2010), separation (Dalili et al. 2019), 3D cell culture (Liu et al. 2017; Kim et al. 2008) and genome amplification (Tian et al. 2018; Panaro et al. 2005). With larger surface area, micropillar arrays as 3D working electrodes have been shown to enhance sensing performance in microchip-based electrochemical detection systems (Chen et al. 2020; Prehn et al. 2011; Liu et al. 2020). Owing to the capillary effect, a well-defined liquid film can be formed between pillars with carefully engineered spacing and aspect ratio in an array (Semperebon et al. 2014), enabling further applications. It has been reported that micropillar arrays, maintaining electrolytes within the pillar zone, can potentially replace microchannels or gels

for electrokinetic separation of proteins to achieve on-chip immunodiagnosis (Li et al. 2010). In previous studies, micropillar arrays with the same wicking effect were used as an ultrashort-pathlength (10–20 μm) cuvette for UV–Vis spectroscopic measurement of high-absorptivity chemicals (Holzner et al. 2015), and as a platform to control the growth of orthorhombic crystals (Holzner et al. 2017). Our recent work has further demonstrated the micropillar arrays as a useful analytical tool to generate spontaneous sample flow and achieve analyte concentration for high-sensitivity measurements (Orlowska et al. 2020). Moreover, micropillar arrays are essential for sorting and separating cells and microparticles in microfluidic systems via the principle of deterministic lateral displacement (Inglis 2009; Chandna and Gundabala 2021). There have also been numerous studies demonstrating that micropillars in a microfluidic chip can help sustain a stable microenvironment for 3D cell culture (Liu et al. 2017; Tomecka et al. 2018). In most cases, the accurate fabrication of the structures is essential for their function. While the fabrication of the aforementioned micropillar arrays was mostly carried out by soft lithography or photolithographic technique with reactive ion etching, the future mass-market need for these microfeature-embedded microfluidic chips has been pressing on manufacturing methods with high production rates. Of these, injection moulding using low-

✉ Craig Priest
craig.priest@unisa.edu.au

¹ Future Industries Institute, UniSA STEM, University of South Australia, Mawson Lakes, SA 5095, Australia

² South Australia Node, Australian National Fabrication Facility, University of South Australia, Mawson Lakes, SA 5095, Australia

cost polymer materials is promising for its ability to mass-produce microdevices (Attia et al. 2009; Maghsoudi et al. 2017).

There have been studies of injection moulding micropillars using thermoplastic polymers such as polypropylene (Weng et al. 2018, 2021; Lu and Zhang 2009), polylactic acid (Yu et al. 2019), polyether-etherketone (PEEK) (Zhang et al. 2016), polyethylene (Zhang et al. 2017), polycarbonate (Zhou et al. 2018a) and other block copolymers (Song et al. 2017; Birkar et al. 2016; Sha et al. 2007). The effects of the process parameters on the moulding process were often the focus of these studies. For example, Li and coworkers have designed and fabricated a disposable blood smart diagnostic chip with an array of micropillars in the flowing channel by injection moulding. They used a styrene acrylic copolymer and investigated the effect of process parameters on the replication quality (Song et al. 2017). A similar structure to micropillars, microneedles were heavily studied for their mass production via injection moulding with polymers such as polycarbonate, PEEK, polystyrene, liquid crystal polymer and so on for the applications in transdermal drug delivery (Juster et al. 2019). These studies particularly highlight the challenge of polymer-filling of microscale features. Successful replication of micro/nano-scale features will continue to be a critical manufacturing requirement as increasingly complex chip designs emerge, and addressing chip material choice will remain an important area of research (Lucchetta et al. 2014; Zhang et al. 2018).

Poly(methyl methacrylate) (PMMA) is a polymer with good mechanical strength and optical properties and is suitable for manufacturing microfluidic devices by injection moulding (Ma et al. 2020). The effect of moulding conditions on the replication of microfeatures on PMMA, including mould temperature, injection velocity (speed), injection pressure/time and packing pressure, have been investigated (Liou and Chen 2006; Chien 2006; Kirchberg et al. 2012). Guided by numerical simulation, there also have been attempts to fabricate nanopillars with PMMA by injection moulding (Jiang et al. 2016; Zhou et al. 2018b). Despite being inadequate in producing nanopillars, these studies have demonstrated the potential of PMMA in moulding micropillars. Cyclic olefin copolymer (COC) is an emerging polymer for injection moulding microstructured polymer parts (Nunes et al. 2010). As a material with low moisture absorption, high optical transparency, resistance to chemical solvents, and biocompatibility, COC has been used to prepare microfluidic devices for DNA stretching (Utiko et al. 2011), DNA detection (Geissler et al. 2020), biomolecular separation (Kourmpetis et al. 2019) and sensing (Prada et al. 2019). A study back in 2011 reported the micro-injection moulding of a lab-on-a-chip device with micropillar features in COC, and yet those

pillars were shallow with an aspect ratio of 1 or much lower (Oh et al. 2011). COC micropillars with an aspect ratio higher than 1 have been prepared using hot embossing (Geissler et al. 2020; Kourmpetis et al. 2019), and there have been studies on the viscosity of COC at high temperatures to help understand the filling of COC during injection moulding (Lu et al. 2020). However, no comparative studies of micropillar array fabrication in PMMA and COC using injection moulding have been reported.

In this paper, we present a systematic study of injection moulding of micropillar arrays using PMMA and COC. The results obtained under different moulding conditions are compared and analysed in conjugation with the physical properties of polymers. COC proves to be more suitable for creating micropillar arrays, compared with PMMA. Furthermore, we show that the nanoroughness of the mould surface is also replicated more completely in COC. With complex microstructures and interfaces critically important in the operation of many microfluidic devices, including those that contain micropillar arrays, the present findings will prove helpful in guiding further development in the mass manufacture of microscale devices via injection moulding.

2 Materials and methods

2.1 Materials

The thermoplastic materials used in this study are PMMA (Altuglas V040) and COC (TOPAS 5013L-10). The PMMA and COC pellets were dried in an oven of 80 °C and 100 °C, respectively, for at least 6 h prior to injection moulding.

2.2 Fabrication of the mould insert

An insert of 6 × 6 microhole arrays (Fig. 1a) was prepared on aluminium 7075-T6 with a Kira SuperMill 2 M computer numerical controlled (CNC) micromilling machine. The tapered holes of 0.25 mm diameter were machined with a Ø0.2 mm HPMT 2 flute end mill (code A02 0020 050 0300 015) at 45,000 rpm in a pecking cycle of 0.05 mm increments to the depth of 0.6 mm and then finished with a HSS (high speed surfacing) CAM operation using the same Ø0.2 mm tool. The cutting parameters were 45,000 rpm spindle speed, 100 mm/min feed rate with a 0.001 mm stepover. The external faces of the insert were machined with a Ø5 mm Kyocera 3 fluted carbide end mill (code 44892), following by standard metallurgical grinding and polishing steps to achieve a better surface finish (40 nm surface roughness) compared to the milled one with a surface roughness of around 120 nm. The extra

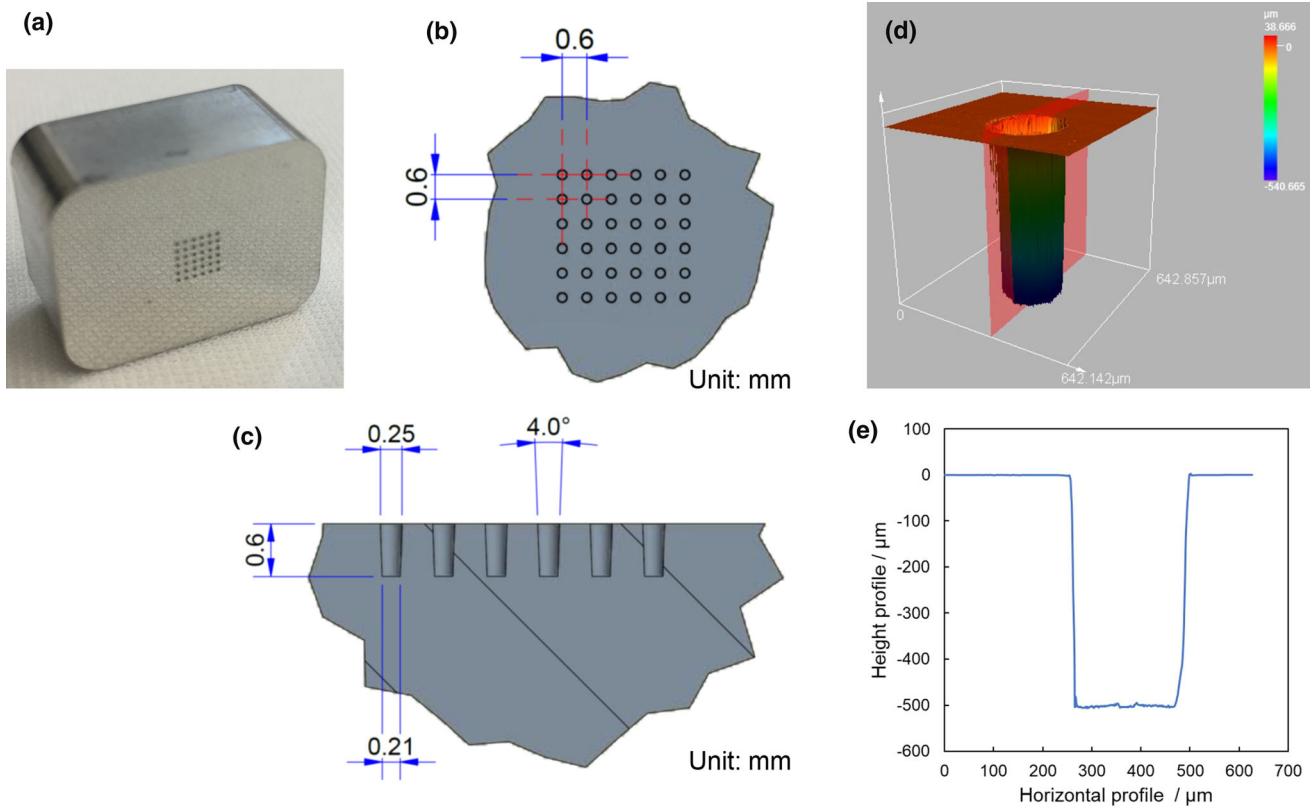


Fig. 1 (a) The mould insert of the microhole array (the inverse form of the micropillar array). The CAD design of the microhole array: top (b) and side (c) schematic views. (d) The 3D profile of one of the

microholes from the insert, measured by an Olympus OLS 5000 confocal microscope. (e) The height profile showing the actual dimension of the microhole

grinding and polishing steps also render a final depth of 0.496 ± 0.006 mm for the holes (Fig. 1e).

The milling parameters of the insert for roughness study and its surface characterisation were described elsewhere (Guan et al. 2019). Briefly, 14 square bosses ($5 \text{ mm} \times 5 \text{ mm} \times 0.1 \text{ mm}$) were milled on the same aluminium 7075-T6 material with Kyocera 4-flute ball nose end mills (code 1835-0315.047 and 1835-0157.024) and Performance Micro Tool 2-flute flat end mills (part number TS-2-0060-S and TS-2-0100-S). The spindle speed was fixed at 49,000 rpm. Other machined parameters including feed rate and depth of cut varied among the bosses to achieve a range of surface roughness from 45 nm up to 174 nm.

2.3 Injection moulding

The injection moulding experiments were performed on a Juken JMW-027S-20t hybrid driven vertical-type moulding machine. The injection moulding conditions for PMMA and COC micropillar parts are listed in Tables 1 and 2, respectively. The injection pressure, holding pressure, injection speed and mould temperature were varied for the mould replication and roughness studies. The moulded

parts were only collected when the moulding parameters were stable after each change of the moulding condition.

2.4 Characterisation

The height of the PMMA and COC micropillars and the surface roughness of COC parts reported as the arithmetic mean height over an area were measured using an Olympus OLS5000 confocal microscope system with a $20 \times$ objective (field of view = 0.41 mm^2). The height of micropillars was averaged from at least three different moulded parts selected at random. The surface roughness was averaged from a total of 6 randomly chosen areas of $644 \mu\text{m} \times 644 \mu\text{m}$ on two separate COC parts. A close examination of the micropillar structure was conducted on the Zeiss Merlin field-emission gun scanning electron microscope with an accelerating voltage of 2–3 kV or the Aspex PSEM eXpress benchtop scanning electron microscope with an accelerating voltage of 20 kV. A 10-nm gold coating (HHV TF500 sputter coater) was applied on the polymer parts to ensure conductivity for imaging.

Table 1 The moulding conditions for PMMA micropillars

Manufacturing parameters	1	2	3	4
Nozzle temperature (°C)	238	238	238	238
Cylinder pre-heat temperature (°C)	235	235	235	235
Cylinder melting temperature (°C)	230	230	230	230
Mould temperature (°C)	95	95	95	105
Injection pressure (MPa)	8–13	12	10	10
Holding pressure (MPa)	8	4–12	10	10
Switching pressure (MPa)	8 (9)	8	8	8
Injection speed (mm/s)	15.6	15.6	40, 50, 60	60–137.5
Injection time (s)	8	8	8	8
Pressure switching time (s)	0.3	0.3	0.3	0.3
Cooling time (s)	9	9	9	9
Eject advance/return time (s)	1/1	1/1	1/1	1/1
Back pressure (MPa)	1	1	1	1

Table 2 The moulding conditions for COC

Manufacturing parameters	1	2	3	4	5
Nozzle temperature (°C)	300	300	300	300	300
Cylinder pre-heat temperature (°C)	295	295	295	295	295
Cylinder melting temperature (°C)	280	280	280	280	280
Mould temperature (°C)	105	105	105	115	105/115
Injection pressure (MPa)	8	9/10	8	8	6
Holding pressure (MPa)	5, 6, 6.5	7	6	6	4.5/5
Switching pressure (MPa)	6	8	6	6	6
Injection speed (mm/s)	27.3	27.3	27.3–120	81.9–120	80, 120
Injection time (s)	8	8	8	8	8
Pressure switching time (s)	0.3	0.3	0.3	0.3	0.3
Cooling time (s)	13	13	13	13	13
Eject advance/return time (s)	1/1	1/1	1/1	1/1	1/1
Back pressure (MPa)	1	1	1	1	1

3 Results and discussion

3.1 PMMA microlenses

Based on the literature (Zhou et al. 2017, 2018b) and preliminary tests, injection pressure and holding pressure (or packing pressure) were identified as two critical parameters in PMMA pillar formation. Two sets of parameters (Columns 1 and 2, Table 1) varying injection pressure and holding pressure, respectively, were tested. Scanning electron microscopy (SEM) images in Fig. 2 revealed PMMA micro-lenses, rather than micropillars, were formed for all parameters studied. Figure 2a shows the average central lens height at different injection pressure and holding pressure measured by the Olympus confocal laser microscope. The lens height is more sensitive to the injection pressure than holding pressure, as one might expect; however, increasing injection pressure also leads to incomplete filling at the root of the micro-lenses (Fig. 2d

and e). The tallest lens was achieved with 12 MPa injection pressure and 9 MPa holding pressure. Nonetheless, the PMMA only fills around 30% of the hole in the mould insert (i.e. the PMMA fills 145 µm into the 496 µm deep hole), which is unsuitable for typical applications of micropillars.

The mould temperature has also been shown to be an effective measure to achieve better micro/nano-feature filling (Jiang et al. 2016). To be comparable to the study of COC moulding, along with the mould temperature, the effect of injection speed on the PMMA filling was also investigated according to the conditions in columns 3 and 4 of Table 1. The filling of the holes was improved with the increase of injection speed, evidenced by the increase of pillar height and the smooth sidewall in Fig. 3. A higher mould temperature of 105 °C saw the further enhancement of the filling behaviour, as it slowed down the solidification of the polymer melt. The best outcome was 50% filling achieved at 100 mm/s injection speed and mould

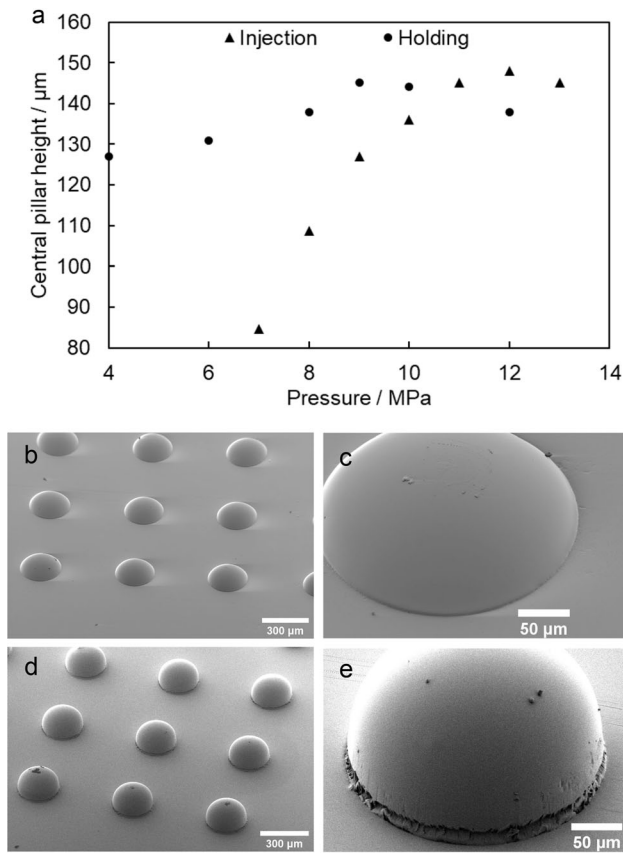


Fig. 2 a The PMMA lens heights under different injection pressure and holding pressure that are specified in the columns 1 and 2 of Table 1. SEM images of moulded PMMA microstructure: micro-lenses with the maximum height of 80 μm (b) moulded under 7 MPa injection pressure and 5.8 MPa holding pressure and its close-up (c); microlenses (d, max height 145 μm) formed under 12 MPa injection pressure and 9 MPa holding pressure and its close-up (e). The tilt angle is 45°

temperature of 105 °C. It confirms again the limitation of using PMMA for micropillar applications, due to its rheological properties, which will be discussed later in the text.

3.2 COC micropillars

As COC has a lower melt viscosity than PMMA, it is expected to have a better filling property than PMMA. Figure 4 shows the moulding results of COC pillars when varying the injection pressure and holding pressure according to parameters in columns 1 and 2 in Table 2. It is found that the injection pressure and holding pressure have only negligible effects on the pillar height. Furthermore, the COC pillar height is significantly larger than observed for similar injection moulding conditions using PMMA.

Yu et al. have noted the effect of injection velocity on the filling behaviours of moulded polylactic acid micropillar

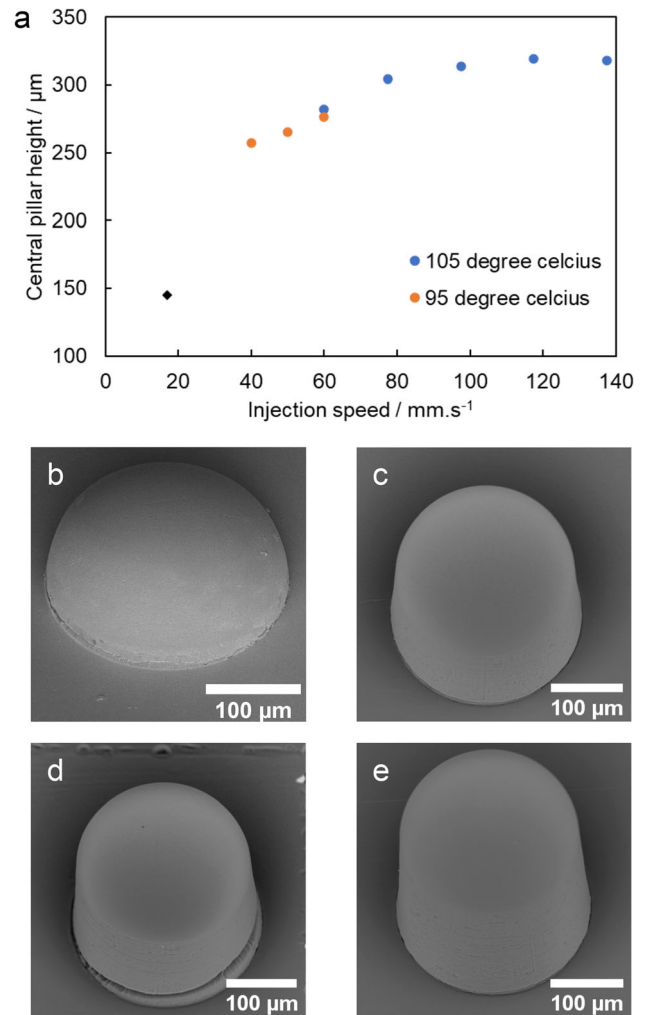


Fig. 3 a The pillar height versus injection speed at different mould temperatures while both injection pressure and holding pressure are 10 MPa. The black diamond indicates the maximum height achieved with the injection speed of 17 mm/s in this study. Note that at 95 °C of mould temperature, the injection speed cannot surpass 60 mm/s due to material overpacking. b–e SEM images of the PMMA micropillars obtained at the injection speed of 17 mm/s, 50 mm/s, 60 mm/s and 100 mm/s, respectively

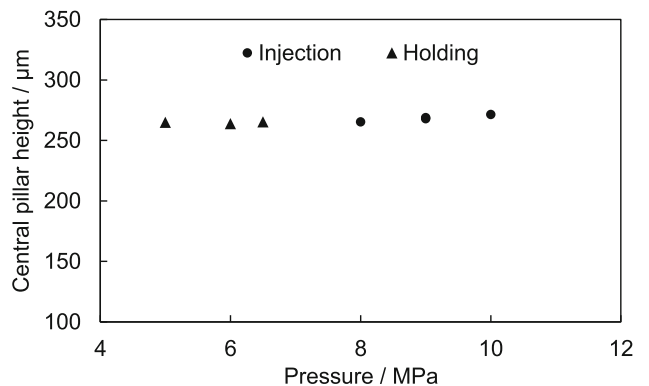


Fig. 4 The effect of injection pressure and holding pressure on the height of COC pillars

array (Yu et al. 2019). Eladl et al. have also reported the most effective parameters in moulding high aspect ratio polymeric micro features being injection speed and holding pressure (Eladl et al. 2018). Hence, diverse injection speeds as shown in column 3 of Table 2 were examined for COC moulding. Figure 5a shows that higher injection speed leads to higher pillars over the range studied. When the injection speed reaches 120 mm/s, full replication of the insert could be achieved. The relationship between injection speed and pillar height suggests that the COC polymer is solidifying too soon at small injection speeds to completely fill the mould. To further improve the filling quality, the mould temperature was increased from 105 to 115 °C (Table 2 Column 4), as the elevation of mould temperature was reported to aid the flow of the melt into microcavities by lowering the viscosity of the

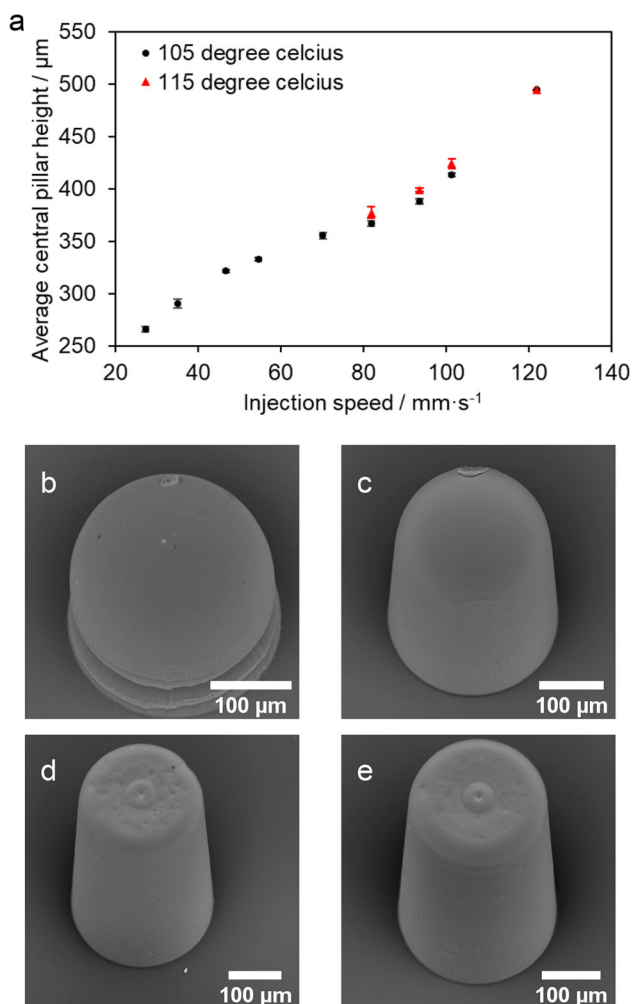


Fig. 5 a The effect of injection speed on the height of COC pillars at two different mould temperatures, 105 °C and 115 °C, while the injection pressure and holding pressure remain at 8 MPa and 6 MPa, respectively. **b–d** SEM images of COC pillars formed with 105 °C of mould temperature at 27.3 mm/s, 100 mm/s, and 120 mm/s injection speeds, respectively. **e** The COC pillar moulded with mould temperature at 115 °C and injection speed at 120 mm/s

polymer melt (Lin et al. 2013). This higher temperature moulding condition can slightly improve the filling evidenced by the marginally increased pillar height shown in Fig. 5a and can also achieve complete filling of the microholes at high injection speed.

SEM examination of the COC parts (Fig. 5b–d) confirms the pillar formation at increasing injection speed. Upon complete filling, the pillar tops are flattened rather than dome-shaped and show the circular feature corresponding to the milling mark from the bottom of the microholes (Fig. 5d and e). The SEM images confirm that the pillars are successfully replicated at high injection speed and there is very little surface roughness or debris present. The overall shape is consistent with typical micropillars applied in microfluidic chips.

As indicated in Fig. 4, the injection pressure and holding pressure have little impact on the pillar height. To further confirm the important role of injection speed in COC pillar moulding, a set of COC parts was shot with the injection pressure of 6 MPa and the holding pressure of 4.5 and 5 MPa (Table 2 Column 5). The laser confocal measurement indicated that with 120 mm/s injection speed, even lower pressure can achieve full pillar replication. The SEM images of these pillars are shown in Fig. 6. Among the COC parts that have achieved full pillar replication, we also investigate the variation in pillar height in the 6 by 6 array. The height of a total of nine pillars distributed evenly at the first, middle and last rows of the array for each COC part was measured. The standard deviation of the pillar height is less than 5 μm, showing a consistent filling across the microhole array.

In summary, COC is able to completely fill the microcavities in the insert, while PMMA only achieves partial filling. Generally, the filling of cavities on a mould insert during injection moulding can be affected by several factors. They are the solidification of hot polymer melt when meeting the relatively cold micro-features of the insert, the pressure drop from the gate to the end of the insert, and the polymer friction on the metallic surface when the size of

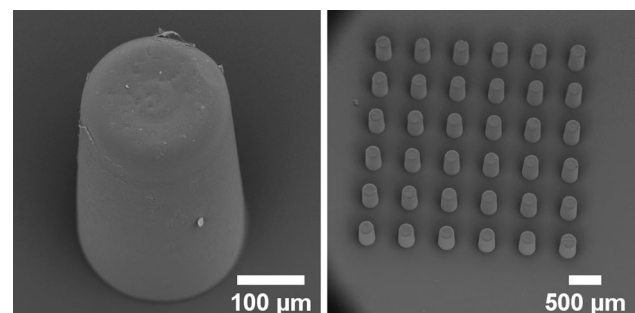


Fig. 6 SEM images of COC pillars formed at the same high injection speed (120 mm/s) and mould temperature (115 °C), but lower injection pressure (6 MPa) and holding pressure (5 MPa)

the feature reduces (Lucchetta et al. 2014; Mélé and Giboz 2018). Some of the effects may be mitigated by changing the moulding conditions or applying anti-stiction coating on the insert to facilitate the polymer flow. However, intrinsically they are associated with polymer properties (Kalima et al. 2007; Theilade and Hansen 2007), that is, how the polymer melt flows and fills under high temperature and pressure. Table 3 lists some of the rheological data of the two polymers studied here. COC has a higher melt flow index and much lower viscosity than PMMA at the set melt temperatures. Thus, a better pillar formation in COC is expected compared to PMMA. It also agrees with our observation that even high injection/holding pressure did not improve the moulding result of PMMA significantly. When the injection speed is high, it alleviates the solidification effect and in turn advances the polymer flow leading to higher pillar formation, which agrees with the results in Fig. 5 for COC. Moreover, COC with the olefin backbone has a contact angle of about 85° and relatively low surface energy to bond with surrounding materials (Choi et al. 2016). In contrast, PMMA is hydrophilic with a contact angle of ~ 70° and high surface energy, due to the presence of carboxylate and methyl ester groups. Therefore, the adhesion force between the polymer and the metallic insert is less for COC than for PMMA, which also promotes the filling of COC to the microholes and avoids the fracture of the moulded pillar (typically in Fig. 2e) during the demolding process.

3.3 Surface roughness of COC parts

The replication of surface roughness is now considered. Referring to our previous report, the replication of insert roughness was limited by the intrinsic roughness of PMMA material (Guan et al. 2019). As the rheological properties of the polymer are crucial for the replication of the mould surface (Quadrini et al. 2020), COC with low viscosity could possibly provide a better surface replication than PMMA. Figure 7 shows the roughness results of COC parts moulded under different injection speeds. The ratio between insert roughness and COC part roughness is approx. 1.5:1 for insert roughness less than 100 nm. This is close to, but not quite, perfect replication (1:1). In our

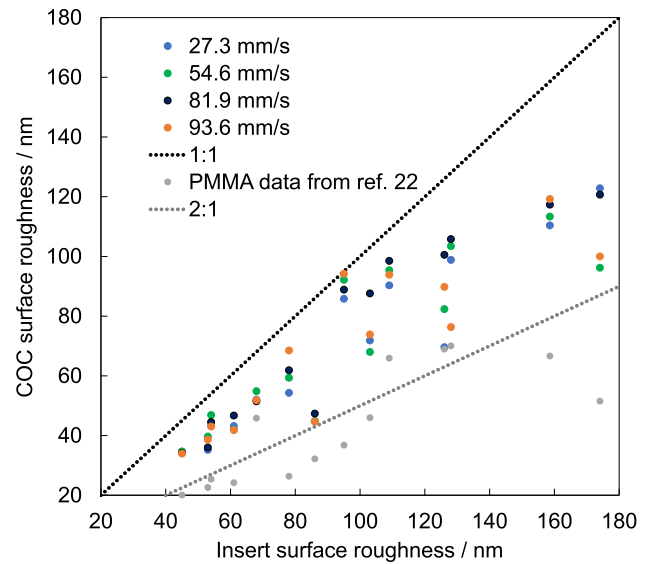


Fig. 7 The surface roughness comparison between the mould insert and the COC part moulded at varied injection speeds

previous study using PMMA, this ratio was closer to 2:1, which is consistent with the pillar moulding results (COC fills micro/nanostructures more effectively). When the effect of injection speed on surface roughness of COC is considered, no significant differences were observed. This is attributed to the small (nanoscale) distances that the polymer melt travels to fill the roughness features, compared with the microholes in which cooling effects are significant.

4 Conclusions

In this paper, we report the injection moulding of micropillars using two thermoplastic polymers of distinct physical and chemical properties, namely PMMA and COC. COC’s lower viscosity leads to more complete filling, compared to PMMA. For low injection speeds (< 100 mm/s) and mould temperature (95 °C for PMMA and 105 °C for COC), we observe lenses or lens-capped pillars, which may be useful in some applications but was not the objective of this work. Increasing injection speed (120 mm/s) and mould temperature (105 °C for PMMA

Table 3 The properties of PMMA and COC used in this study

	PMMA (Altuglas V040)	COC (TOPAS 5013L-10)
Glass transition temperature (T _g /°C)	95	130
Melt flow index	3.5 g/10 min (230 °C–3.8 kg)	47 g/10 min (260 °C–2.16 kg) (Sahli et al. 2004)
Viscosity, η (Pa s, at the shear rate of 100 s ⁻¹)	> 300 at 230 °C (Xu et al. 2011)	~ 100 at 280 °C (Lu et al. 2020)

and 115 °C for COC) slightly improved the filling for PMMA and achieved complete filling (flat-topped pillars) for COC. The latter resembles pillars that are used in a variety of microfluidic devices. Moreover, full replication of the microholes with COC can be achieved at much lower injection pressure and holding pressure (6 MPa and 4.5 MPa). Finally, replication of nanoscale surface roughness was improved for COC compared with PMMA, suggesting that COC may offer advantages for injection moulding complex nano/microfluidic devices and interfaces.

Acknowledgements Funding from the Australian Academy of Science, on behalf of the Department of Industry, Innovation and Science is gratefully acknowledged. The Regional Collaborations Programme is supported by the Australian Government under the National Innovation and Science Agenda. This work was performed in part at the South Australian node of the Australian National Fabrication Facility (ANFF-SA), which is supported by Australia's National Collaborative Research Infrastructure Strategy (NCRIS).

Funding Open Access funding enabled and organized by CAUL and its Member Institutions.

Declarations

Conflict of interest No competing interests.

Open Access This article is licensed under a Creative Commons Attribution 4.0 International License, which permits use, sharing, adaptation, distribution and reproduction in any medium or format, as long as you give appropriate credit to the original author(s) and the source, provide a link to the Creative Commons licence, and indicate if changes were made. The images or other third party material in this article are included in the article's Creative Commons licence, unless indicated otherwise in a credit line to the material. If material is not included in the article's Creative Commons licence and your intended use is not permitted by statutory regulation or exceeds the permitted use, you will need to obtain permission directly from the copyright holder. To view a copy of this licence, visit <http://creativecommons.org/licenses/by/4.0/>.

References

- Attia UM, Marson S, Alcock JR (2009) Micro-injection moulding of polymer microfluidic devices. *Microfluid Nanofluid* 7:1
- Birkar S, Mendible G, Park J-G, Mead JL, Johnston SP, Barry CMF (2016) Effect of feature spacing when injection molding parts with microstructured surfaces. *Polym Eng Sci* 56:1330–1338
- Chandna P, Gundabala V (2021) Pillar based microfluidic approach to sorting of microparticle mixtures at various particle ratios. *Microfluid Nanofluid* 25:6
- Chen C, Ran B, Wang Z, Zhao H, Lan M, Chen H et al (2020) Development of micropillar array electrodes for highly sensitive detection of biomarkers. *RSC Adv* 10:41110–41119
- Chien R-D (2006) Micromolding of biochip devices designed with microchannels. *Sens Actuators, A* 128:238–247
- Choi SY, Habimana O, Flood P, Reynaud EG, Rodriguez BJ, Zhang N et al (2016) Material- and feature-dependent effects on cell adhesion to micro injection moulded medical polymers. *Colloids Surf, B* 145:46–54
- Dalili A, Samiei E, Hoorfar M (2019) A review of sorting, separation and isolation of cells and microbeads for biomedical applications: microfluidic approaches. *Analyst* 144:87–113
- Eladl A, Mostafa R, Islam A, Loaldi D, Soltan H, Hansen HN et al (2018) Effect of process parameters on flow length and flash formation in injection moulding of high aspect ratio polymeric micro features. *Micromachines* 9:58
- Geissler M, Malic L, Morton KJ, Clime L, Daoud J, Hernández-Castro JA et al (2020) Polymer micropillar arrays for colorimetric DNA detection. *Anal Chem* 92:7738–7745
- Guan B, Cherrill M, Pai J-H, Priest C (2019) Effect of mould roughness on injection moulded poly (methyl methacrylate) surfaces: roughness and wettability. *J Manuf Process* 48:313–319
- Holzner G, Kriel FH, Priest C (2015) Pillar cuvettes: capillary-filled, microliter quartz cuvettes with microscale path lengths for optical spectroscopy. *Anal Chem* 87:4757–4764
- Holzner G, Binder C, Kriel FH, Priest C (2017) Directed growth of orthorhombic crystals in a micropillar array. *Langmuir* 33:1547–1551
- Inglis DW (2009) Efficient microfluidic particle separation arrays. *Appl Phys Lett* 94:013510
- Jiang B-Y, Zhou M-Y, Weng C, Zhang L, Lv H (2016) Fabrication of nanopillar arrays by combining electroforming and injection molding. *Int J Adv Manuf Technol* 86:1319–1328
- Juster H, van der Aar B, de Brouwer H (2019) A review on microfabrication of thermoplastic polymer-based microneedle arrays. *Polym Eng Sci* 59:877–890
- Kalima V, Pietarinen J, Siitonen S, Immonen J, Suvanto M, Kuitinen M et al (2007) Transparent thermoplastics: Replication of diffractive optical elements using micro-injection molding. *Opt Mater* 30:285–291
- Kim MS, Hwang H, Choi Y-S, Park J-K (2008) Microfluidic micropillar arrays for 3D cell culture. *Open Biotechnol J* 2:224–228
- Kirchberg S, Chen L, Xie L, Ziegmann G, Jiang B, Rickens K et al (2012) Replication of precise polymeric microlens arrays combining ultra-precision diamond ball-end milling and micro injection molding. *Microsyst Technol* 18:459–465
- Kourmpetis I, Kastania AS, Ellinas K, Tsougeni K, Baca M, De Malsche W et al (2019) Gradient-temperature hot-embossing for dense micropillar array fabrication on thick cyclo-olefin polymeric plates: an example of a microfluidic chromatography column fabrication. *Micro Nano Eng* 5:100042
- Li H-Y, Dauriac V, Thibert V, Senechal H, Peltre G, Zhang X-X et al (2010) Micropillar array chips toward new immunodiagnosis. *Lab Chip* 10:2597–2604
- Lin H-L, Chen C-S, Lee R-T, Chen S-C, Chien R-D, Jeng M-C et al (2013) Effects of process parameters on replication accuracy of microinjection molded cyclic olefins copolymers parts. *Jpn J Appl Phys* 52:044001
- Liou AC, Chen RH (2006) Injection molding of polymer micro- and sub-micron structures with high-aspect ratios. *Int J Adv Manuf Technol* 28:1097–1103
- Liu J-S, Zhang Y-Y, Wang Z, Deng J-Y, Ye X, Xue R-Y et al (2017) Design and validation of a microfluidic chip with micropillar arrays for three-dimensional cell culture. *Chin J Anal Chem* 45:1109–1114
- Liu B, Lv C, Chen C, Ran B, Lan M, Chen H et al (2020) Electrochemical performance of micropillar array electrodes in microflows. *Micromachines* 11:858
- Lu Z, Zhang KF (2009) Morphology and mechanical properties of polypropylene micro-arrays by micro-injection molding. *Int J Adv Manuf Technol* 40:490–496

- Lu J, Qiang Y, Wu W, Jiang B (2020) Experimental study on viscosity properties of cyclic olefin copolymer (COC) flowing through micro capillary dies. *Polym Testing* 89:106635
- Lucchetta G, Sorgato M, Carmignato S, Savio E (2014) Investigating the technological limits of micro-injection molding in replicating high aspect ratio micro-structured surfaces. *CIRP Ann* 63:521–524
- Ma X, Li R, Jin Z, Fan Y, Zhou X, Zhang Y (2020) Injection molding and characterization of PMMA-based microfluidic devices. *Microsyst Technol* 26:1317–1324
- Maghsoudi K, Jafari R, Momen G, Farzaneh M (2017) Micro-nanostructured polymer surfaces using injection molding: a review. *Mater Today Commun* 13:126–143
- Mélé P, Giboz J (2018) Micro-injection molding of thermoplastic polymers: proposal of a constitutive law as function of the aspect ratios. *J Appl Polym Sci* 135:45719
- Nunes PS, Ohlsson PD, Ordeig O, Kutter JP (2010) Cyclic olefin polymers: emerging materials for lab-on-a-chip applications. *Microfluid Nanofluid* 9:145–161
- Oh H, Park J, Song Y, Youn J (2011) Micro-injection moulding of lab-on-a-chip (LOC). *Ann Trans Nord Rheol Soc* 19:1–9
- Orlowska MK, Guan B, Sedev R, Morikawa Y, Suu K, Priest C (2020) Evaporation-driven flow in micropillar arrays: transport dynamics and chemical analysis under varied sample and ambient conditions. *Anal Chem* 92:16043–16050
- Panaro NJ, Lou XJ, Fortina P, Kricka LJ, Wilding P (2005) Micropillar array chip for integrated white blood cell isolation and PCR. *Biomol Eng* 21:157–162
- Prada J, Cordes C, Harms C, Lang W (2019) Design and manufacturing of a disposable, cyclo-olefin copolymer, microfluidic device for a biosensor. *Sensors* 19:1178
- Prehn R, Abad L, Sánchez-Molas D, Duch M, Sabaté N, del Campo FJ et al (2011) Microfabrication and characterization of cylinder micropillar array electrodes. *J Electroanal Chem* 662:361–370
- Quadrini F, Bellisario D, Santo L, Bottini L, Boschetto A (2020) Mold replication in injection molding of high density polyethylene. *Polym Eng Sci* 60:2459–2469
- Sahli M, Roques-Carnes C, Malek CK, Duffait R (2004) Study of the rheological properties of poly(methylmethacrylate) (PMMA) and cyclo-olefin-copolymer (COC) to optimize the hot-embossing process. In: Menz W, Dimov S (eds) *Multi-material micro manufacture*. Elsevier, Amsterdam
- Semprebon C, Forsberg P, Priest C, Brinkmann M (2014) Pinning and wicking in regular pillar arrays. *Soft Matter* 10:5739–5748
- Sha B, Dimov S, Griffiths C, Packianather MS (2007) Investigation of micro-injection moulding: factors affecting the replication quality. *J Mater Process Technol* 183:284–296
- Song M, Zhao H, Liu J, Liu C, Li J (2017) Replication of large scale micro pillar array with different diameters by micro injection molding. *Microsyst Technol* 23:2087–2096
- Theilade UA, Hansen HN (2007) Surface microstructure replication in injection molding. *Int J Adv Manuf Technol* 33:157–166
- Tian HC, Benitez JJ, Craighead HG (2018) Single cell on-chip whole genome amplification via micropillar arrays for reduced amplification bias. *PLoS ONE* 13:e0191520
- Tomecka E, Zukowski K, Jastrzebska E, Chudy M, Brzozka Z (2018) Microsystem with micropillar array for three- (gel-embaded) and two-dimensional cardiac cell culture. *Sens Actuators, B Chem* 254:973–983
- Utiko P, Persson F, Kristensen A, Larsen NB (2011) Injection molded nanofluidic chips: fabrication method and functional tests using single-molecule DNA experiments. *Lab Chip* 11:303–308
- Weng C, Wang F, Zhou M, Yang D, Jiang B (2018) Fabrication of hierarchical polymer surfaces with superhydrophobicity by injection molding from nature and function-oriented design. *Appl Surf Sci* 436:224–233
- Weng C, Sun H, Lai J, Liu J, Zhai Z (2021) Experimental investigation and molecular dynamics simulations of the effect of processing parameters on the filling quality of injection-molded micropillars. *Polym Eng Sci* 1:1–10
- Xu B, Lu YB, Li GM, Xue S, Xiang BP (2011) Rheological behavior of polymethyl methacrylate (PMMA) filling through micro channels. *Adv Mater Res* 189–193:451–454
- Yu W, Ruan S, Li Z, Gu J, Wang X, Shen C et al (2019) Effect of injection velocity on the filling behaviors of microinjection-molded polylactic acid micropillar array product. *Int J Adv Manuf Technol* 103:2929–2940
- Zhang Y, Hansen HN, Sørensen S (2016) Injection molding of micro pillars on vertical side walls using polyether-ether-ketone (PEEK). In: *Proceeding of 11th international conference on micro manufacturing*. Paper 16
- Zhang Y, Pedersen DB, Gøtje AS, Mischkot M, Tosello G (2017) A soft tooling process chain employing additive manufacturing for injection molding of a 3D component with micro pillars. *J Manuf Process* 27:138–144
- Zhang H, Fang F, Gilchrist MD, Zhang N (2018) Filling of high aspect ratio micro features of a microfluidic flow cytometer chip using micro injection moulding. *J Micromech Microeng* 28:075005
- Zhou M, Jiang B, Weng C, Zhang L (2017) Experimental study on the replication quality of micro–nano cross-shaped structure arrays in injection molding. *Microsyst Technol* 23:983–989
- Zhou M, Xiong X, Jiang B, Weng C (2018a) Fabrication of high aspect ratio nanopillars and micro/nano combined structures with hydrophobic surface characteristics by injection molding. *Appl Surf Sci* 427:854–860
- Zhou M, Xiong X, Drummer D, Jiang B (2018b) Molecular dynamics simulation and experimental investigation of the geometrical morphology development of injection-molded nanopillars on polymethylmethacrylate surface. *Comput Mater Sci* 149:208–216

Publisher's Note Springer Nature remains neutral with regard to jurisdictional claims in published maps and institutional affiliations.